J Mater Sci (2011) 46:2365–2369
DOI 10.1007/s10853-010-5083-2

Corrosion behavior in SBF for titania coatings on Mg–Ca alloy

Meiheng Li · Qian Chen · Wenjin Zhang · Wangyu Hu · Yong Su

Received: 20 August 2010 / Accepted: 12 November 2010 / Published online: 30 November 2010

Abstract TiO_2 coating was obtained by sol–gel method to improve the corrosion resistance of Mg–Ca alloy in human body environment. The corrosion behavior of Mg–1.0 Ca alloy with TiO_2 coating was investigated by electrochemical tests and immersion tests in simulated body fluid (SBF). Bare Mg–1.0 Ca alloy suffered serious attack after immersed in simulated body fluid only for 48 h. While for the Mg–1.0 Ca alloy with TiO_2 coating, the surface almost maintained intact with only several collapses after immersed in SBF for 168 h. The electrochemical test results showed that the free corrosion current (i_{corr}) of Mg–1.0 Ca alloy substrate was 3.3275e−2A/cm^2, while the i_{corr} of TiO_2 coating was only 1.58549e−5A/cm^2. Therefore, TiO_2 coating significantly improved the corrosion resistance of Mg–1.0 Ca alloy in SBF. This enhances the potential of Mg–Ca alloy used as biodegradable orthopedic material.

Introduction

As potential biodegradable materials, magnesium alloys show many advantages over current metallic materials, and biodegradable plastics and ceramics [1]. Among the alloying elements of biodegradable magnesium alloys, calcium is a major component of human bone. The incorporation of magnesium and calcium into bone might be expected to be beneficial to the bone healing with the co-releasing of Mg and Ca ions [2]. In addition, Mg–Ca alloys have a similar density to bone, and recently have gained widespread attention as new biodegradable orthopedic materials [2–4]. However, in aqueous solution, especially for that containing chloride ion like human body fluid, the corrosion rate of Mg–Ca alloys is very high [1]. Mg–Ca alloys cannot maintain sufficient mechanical integrity in the bony union period [1, 5]. The rapid corrosion rate of Mg–Ca alloys in human bio-environment is one of the greatest limitations for its use in biodegradable orthopedic applications [1].

Recently, some researches have been done to slow down the biodegradation rate of magnesium alloys, including PLGA or poly(lactide-co-glycolide) coating [6], plasma electrolytic oxidation composite coating [7], fluoride conversion coating [8], cerium electrolysis treatment [9], sol–gel[10], alkali-heat treatment [11], and plasma immersion ion implantation [12].

TiO_2 is non-toxic and chemically stable and can be used to improve the biocompatibility of the substrate. The resistance to corrosion was obviously improved for the titanium substrate with TiO_2 coating [13–16]. Moreover, TiO_2 coated on Ti scaffolds displays excellent bone-like apatite forming ability and can be anticipated as promising implant materials for orthopedic applications [15]. In this article, TiO_2 was deposited on magnesium calcium alloy by sol–gel to improve the corrosion resistance.

Experimental procedures

Mg–1.0 Ca alloys were prepared from high purity magnesium (99.99 wt%) and calcium particles (99.8 wt%). For the preparation of the TiO_2 sol [15], a tetrabutylorthotitanate ($C_{16}H_{36}TiO_4$) was first diluted with absolute ethanol,

M. Li (✉) · Q. Chen · W. Zhang · W. Hu
Department of Applied Physics, Hunan University, Changsha 410082, China
e-mail: mhli2003@163.com

Y. Su
Hengyang Meteorological Bureau, Hengyang 421001, China

and then a small amount of distilled water mixed with diethanolamine ($NH(CH_2CH_2OH)_2$) was added for hydrolysis, followed by vigorous stirring for 24 h. Subsequently, the mixed sol was aged for 24 h. The TiO_2 layer was coated by a dipping-coating method at a speed of 12 cm/min, followed by a heat treatment at 500 °C for 2 h. The process was repeated several times to obtain a thicker coating.

The corrosion resistance was evaluated by electrochemical tests and immersion tests in the simulated body fluid (SBF), which was prepared according to the procedure described by Kokubo [17]. Electrochemical tests were carried out at 37 °C using a three-electrode cell with a saturated calomel as a reference, a platinum plate as the counter and the specimen as the working electrode. Specimens with 20 × 10 × 2 mm were machined from the ingots and were molded into epoxy resin with only one side of 10 × 20 mm^2 exposed for the test. The working surface was ground, polished, and cleaned in acetone. Before the measurement, the specimens were exposed to the test solution and stabilized for 5 min. Immersion tests were done in SBF for 48, 168, and 336 h. The temperature of SBF was maintained at (37 ± 0.5) °C using water bath and the pH was adjusted to 7.4.

The coating structures were analyzed using D500 XRD. The surface morphologies were observed with S4800 SEM. Microstructure characterization studies were conducted on polished specimens using an optical microscope.

Results and discussion

Figure 1 shows the XRD pattern and metallographical image of the Mg–1.0 Ca alloy. The XRD patterns show very strong diffraction peaks of Mg with some diffraction peaks of Mg_2Ca which can be indexed to the (103), (112), and (313) reflections, suggesting the prepared Mg–1.0 Ca alloy consisted principally of Mg with some Mg_2Ca second phase. The metallographical image shows the distribution and the morphology of the second phases in the Mg–1.0 Ca alloy (Fig. 1b). The second phases mainly distributed along grain boundary in eutectic (Mg + Mg_2Ca), and some small second phase precipitates were also found in the inner grain as shown in Fig. 1b.

Figure 2 shows XRD pattern and the surface morphology of the sol–gel derived TiO_2 coating. The XRD patterns (Fig. 2a) showed strong diffraction peaks of anatase phase, however, very weak diffraction peaks of rutile phase were also observed, indicating that the sol–gel derived TiO_2 coating consisted of mainly anatase phase with trace of rutile phase. Xu [15] reported that the sol–gel derived TiO_2 shows different phases at different annealed temperature. At 340 °C or below, TiO_2 shows amorphous; when the annealed temperature elevated, TiO_2 shows primary anatase structure. With the annealed temperature further elevated, rutile becomes the main phase of the TiO_2 coating, which was transformed from anatase [15]. Therefore, the rutile phase existed in our prepared coating may be transformed from the anatase phase during the heat treatment.

Almost uniformly distributed cracks were observed on the sol–gel TiO_2 coating surface due to the built-up of stresses (Fig. 2b), which were mainly resulted from the effect of thermal-expansion coefficient mismatch between the TiO_2 coating and the substrate after heat treatment. However, the observed surface cracks were not connected with the substrate directly because the cracks in sub-coating were always filled in the repeated dipping-coating process, which was proved by XRD results with no magnesium diffraction peaks (Fig. 2a).

Generally, in the process of electrochemical corrosion, the cathodic polarization curves are assumed to represent the cathodic hydrogen evolution through solution reduction, while the anodic polarization curves represent the dissolution of magnesium alloy [18]. The anodic

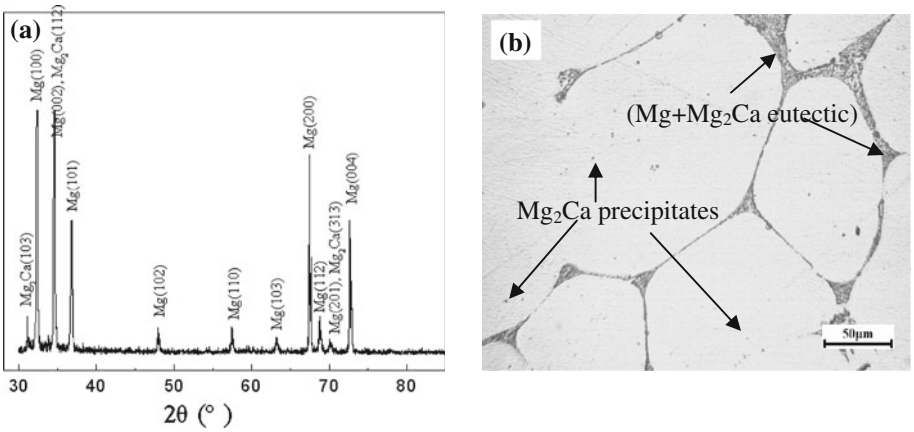

Fig. 1 **a** XRD pattern and **b** optical metallographical image of the Mg–1.0 Ca alloy, showing the morphology of the eutectic (Mg + Mg_2Ca) and the Mg_2Ca precipitates

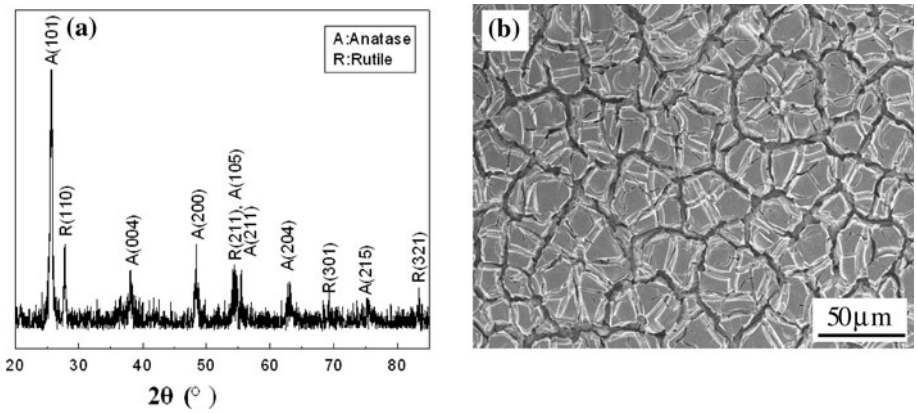

Fig. 2 **a** XRD pattern and **b** surface SEM image of the as-prepared TiO_2 coating, showing lots of cracks on the surface

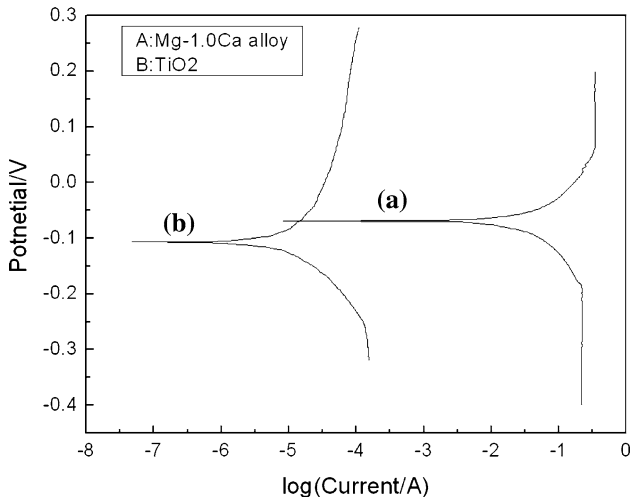

Fig. 3 Potentiodynamic curves of (*a*) Mg–1.0 Ca alloy and (*b*) Mg–1.0 Ca alloy with TiO_2 coating immersed in SBF

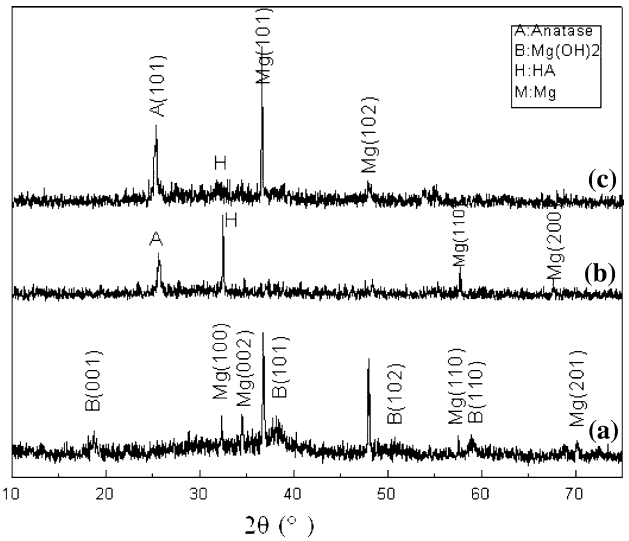

Fig. 4 XRD patterns of Mg–1.0 Ca alloy immersed in SBF for 48 h (*a*) and Mg–1.0 Ca alloy with TiO_2 coating immersed in SBF for (*b*) 168 h, and (*c*) 336 h

polarization curves include the potential smooth phase and the potential rapidly rise phase. When the potential smooth phase is longer, it means the corrosion resistance is better.

Figure 3 shows the potentiodynamic curves of Mg–1.0 Ca alloy without and with TiO_2 coating immersed in SBF. It could be seen that the corrosion current density for Mg–1.0 Ca alloy substrate increased quickly at the beginning of anodic side. Then the diffusion-controlled anodic current behavior was observed at the end of the curves due to the fast corrosion rate [19]. As for the TiO_2 coating specimen, the anodic current density increased more slowly. The free corrosion potential (E_{corr}) values showed that TiO_2 coating on magnesium alloy shifted the corrosion potential toward noble direction and the E_{corr} shift was about 50 mV. While the free corrosion current (i_{corr}) for the TiO_2 coating (1.58549e−5A/cm^2) was lower than that of Mg–1.0 Ca alloy substrate (3.3275e−2A/cm^2) with almost 3 order of factor. It could also be seen that the anodic polarization curve of the TiO_2 coating was much longer than that of Mg–1.0 Ca alloy substrate (Fig. 3). The much lower i_{corr} together with the longer anodic polarization curve and more negative E_{corr} implied that the corrosion resistance was improved for Mg–1.0 Ca alloy with TiO_2 coating in SBF.

Figure 4 shows the XRD patterns of Mg–1.0 Ca alloy immersed in SBF for 48 h and Mg–1.0 Ca alloy with TiO_2 coating immersed in the SBF for 168 and 336 h, respectively. $Mg(OH)_2$ diffraction peaks were found for the Mg–1.0 Ca alloy immersed in SBF for 48 h (Fig. 4a). While for the case of the Mg–1.0 Ca alloy substrate with TiO_2 coating, dominant anatase and trace of hydroxyapatite (HA) phases were detected for the specimen immersed in SBF for 48 h. With the increase of the immersed time (specimen immersed in SBF for 168 h), HA diffraction peaks became more obvious (Fig. 4b), however, very weak diffraction peaks of Mg were also found. With further increase of the immersed time (specimen immersed in SBF for 336 h), the diffraction peaks of anatase and HA phases became weak, while magnesium became the dominant phase (Fig. 4c).

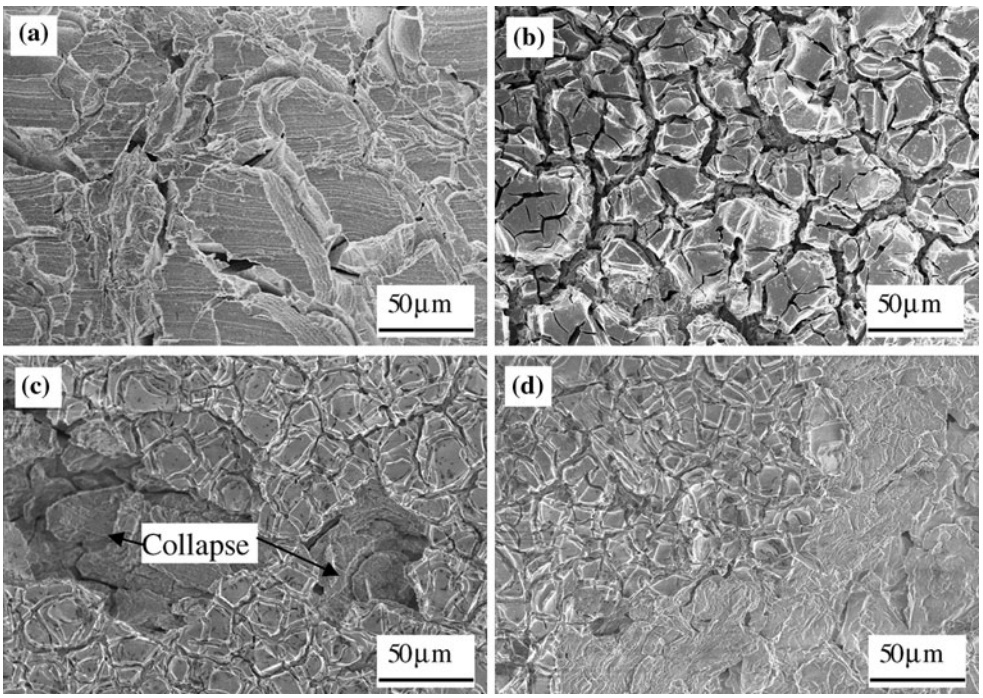

Fig. 5 Corrosion morphologies of Mg–1.0 Ca alloy immersed in SBF for 48 h **a** and Mg–1.0 Ca alloy with TiO_2 coating immersed in SBF for **b** 48 h, **c** 168 h, and **d** 336 h

The SEM images of the surface morphologies for the Mg–1.0 Ca alloy substrate and the TiO_2 coating after immersed in SBF for different time are shown in Fig. 5. After immersed in SBF for 48 h, Mg–1.0 Ca alloy substrate suffered serious attack and many cracks could be observed in the surface (Fig. 5a). While for the specimen with TiO_2 coating after immersed in SBF for 48 h, the surface maintained integrity (Fig. 5b) and the morphology was similar to that of the as-prepared coating (Fig. 2a). As for the specimen with TiO_2 coating after immersed in SBF for 168 h, most of the coating surface kept the same morphology, though several collapses were observed in some area (Fig. 5c). For the specimen with TiO_2 coating after immersed in SBF for 336 h, large corrosion area occurred (Fig. 5d). This was different from the result of the case of TiO_2 coated on Ti substrate. In Ti substrate case, TiO_2 coating maintained integrity even after immersed in SBF for 720 h.

In this study, Mg–1.0 Ca alloy substrate suffered serious attack only immersed in SBF for 48 h (Fig. 5a). Nevertheless, the corrosion resistance was improved for the Mg–1.0 Ca alloy with TiO_2 coatings, and some bioactive HA phase also formed on the surface (Fig. 4b).

In the SBF, OH^- easily bonds to the Ti^+ of TiO_2 and forms Ti–OH groups [14]. At the electrolyte pH < 4, the following reaction takes place on the surface of the coating:

$$\text{Ti}-\text{OH(basic hydroxide)} + \text{H}_2\text{O} \leftrightarrow [\text{Ti}-\text{OH}_2]^+ + \text{OH}^-. \quad (1)$$

So $[\text{Ti–OH}_2]^+$ is produced in the surface layer and makes a positive surface charge. Whereas at the electrolyte pH > 9, Ti–OH gives off proton and becomes $[\text{Ti–OH}]^-$ causing a negative surface charge, and the reaction takes place as follows:

$$\text{Ti}-\text{OH(acidic hydroxide)} + \text{H}_2\text{O} \leftrightarrow [\text{Ti}-\text{O}]^- + \text{H}_3\text{O}^+. \quad (2)$$

While at the electrolyte pH between 4 and 9, both acidic and basic hydroxides coexist on the Ti surface.

With TiO_2 coating specimen immersed in the SBF, calcium and phosphate ions can be absorbed on the sample surface, and the firstly formed Ca–P crystal nuclei is octacalcium phosphate phase ($Ca_8H_2(PO_4)_6{\cdot}5H_2O$), which is a potential precursor of biological apatite crystals in the bones and teeth [20]. The Ti–OH groups induce apatite nucleation, and the released Na^+, Ca^{2+} or K^+ ions accelerate apatite nucleation by increasing the ionic activity product of apatite in the SBF [13, 21]. Once the apatite nuclei are formed, these nuclei can grow spontaneously by consuming the calcium and phosphate ions in the surrounding SBF. The Ti–OH groups are effective for the bone-like apatite formation. And the bone-like apatite layer tends to convert to a Ca-deficient HA in vitro because of

the favored thermodynamics. In this study, HA was detected on the TiO_2 coating after immersed in SBF (Fig. 4b). HA is favorable for implants [21].

However, some SBF solution still penetrated through the TiO_2 coating down to substrate via sub-coating cracks, though the coating surface cracks were not connected with the substrate directly. The penetrated SBF solution easily reacted to Mg–1.0 Ca alloy substrate and its oxide, leading to the local collapse of the TiO_2 coating (Fig. 5c). And so some very weak Mg diffraction peaks were observed in XRD (Fig. 4b). Subsequently, accelerated corrosion in theTiO_2 coating collapse areas resulted in more and more TiO_2 coating peeled off. With further immersed in SBF, large corrosion area occurred (Fig. 5d).

Conclusions

The corrosion behavior of TiO_2 coating depostited on Mg–1.0 Ca alloy by sol–gel method was evaluated through electrochemical measurement and immersion test in SBF. Based on the experimental investigation, the following conclusions can be made.

1. The sol–gel derived TiO_2 coating consisted of mainly anatase phase with trace of rutile phase.
2. The i_{corr} of TiO_2 coating was almost 3 order of factor lower than that of bare Mg–1.0 Ca alloy substrate.
3. The corrosion resistance was improved significantly for the Mg–1.0 Ca alloy with TiO_2 coatings.
4. The application of TiO_2 coatings enhances the potential of Mg–Ca alloy as biodegradable implants.

Acknowledgements This work was supported by Hunan Provincial Natural Science Foundation of China (10JJ3073).

References

1. Staiger MP, Pietak AM, Huadmai J, Dias G (2006) Biomaterials 27:1728
2. Li Z, Gu X, Lou S, Zheng Y (2008) Biomaterials 29:1329
3. Yun Y, Dong Z, Yang D, Schulz MJ, Shanov VN, Yarmolenko S, Xu Z, Kumta P, Sfeir C (2009) Mater Sci Eng C 29:1814
4. Pietak A, Mahoney P, Dias GJ, Staiger MP (2008) J Mater Sci Mater Med 19:407
5. Witte F, Feyerabend F, Maier P, Fischer J, Stormer M, Blawert C, Dietzel W, Hort N (2007) Biomaterials 28:2163
6. Li JN, Cao P, Zhang XN, Zhang SX, He YH (2010) J Mater Sci 45:6038. doi:10.1007/s10853-010-4688-9
7. Guo J, Wang LP, Wang SC, Liang J, Xue QJ, Yan FY (2009) J Mater Sci 44:1998. doi:10.1007/s10853-009-3291-4
8. Chiu KY, Wong MH, Wong FT, Wong HC (2007) Surf Coat Technol 202:590
9. Sun HH, Li XF, Chen D, Wang HW (2009) J Mater Sci 44:786. doi:10.1007/s10853-008-3133-9
10. Zhang XZ, Zhou J, Wang JD, Jiang YH (2009) J Mater Sci 44:2938. doi:10.1007/s10853-009-3389-8
11. Li LC, Li JC, Li Y (2007) Surf Coat Technol 185:92
12. Liu CL, Liu YC, Tian XB, Tian PK (2007) Thin Solid Films 516:422
13. Wen CE, Xu W, Hu WY, Hodgson PD (2007) Acta Biomater 3:403
14. Ma QQ, Li MH, Hu ZY, Chen Q, Hu WY (2008) Mater Lett 62:3035
15. Xu W, Hu WY, Li MH, Wen CE (2006) Mater Lett 60:1575
16. Sun CW, Hui R, Qu W, Yick S, Sun C, Qian WM (2010) J Mater Sci 45:6235. doi:10.1007/s10853-010-4718-7
17. Kokubo T, Takadama H (2006) Biomaterials 27:2907
18. Chang JW, Guo XW, Fu PH, Peng LM, Ding WJ (2007) Electrochima Acta 52:3160
19. Cao CN (2004) Principle of erosive electrochemistry. Chemical Industry Press, China, p 243
20. Lu X, Leng Y (2005) Biomaterials 26:1097
21. Hsu HC, Wu SC, Fu CL, Ho WF (2010) J Mater Sci 45:3661. doi:10.1007/s10853-010-4411-x